ELSEVIER

Earth and Planetary Science Letters 201 (2002) 593–607

EPSL

www.elsevier.com/locate/epsl

Experimental evidence for the pressure dependence of fission track annealing in apatite

Anke S. Wendt [a,b,*], Olivier Vidal [c,1], Lewis T. Chadderton [d]

[a] *Heidelberger Akademie der Wissenschaften am Max Planck Institut für Kernphysik, Abteilung Archäometrie, Saupfercheckweg 1, 69117 Heidelberg, Germany*

[b] *Laboratoire de Géophysique, Tectonique et Sédimentologie, ISTEEM, Université Montpellier 2, Place, Eugène Bataillon, 34095 Montpellier, France*

[c] *Laboratoire de Géologie, Département Terre, Atmosphère et Océans, Ecole Normale Supérieure, 24 rue Lhomond, 75005 Paris, France*

[d] *Atomic and Molecular Physics Laboratories, Research School of Physical Sciences and Engineering, Institute for Advanced Studies, Australian National University, Canberra, ACT 0020, Australia*

Received 11 January 2002; received in revised form 22 March 2002; accepted 17 May 2002

Abstract

Fission track analysis has seen a major expansion in application to general geological problems reflecting its advances in understanding the temperature dependence of track annealing and track length distributions. However, considerable uncertainties still persist, in particular concerning the stability of fission tracks subjected to the interaction of environmental physical parameters (e.g. pressure, temperature, stress) and in extrapolation of laboratory data to geological time scales. In this work, we studied the fading behavior of spontaneous fission tracks in basic apatite [hexagonal $Ca_5(PO_4)_3(OH, F, Cl)$] when exposed simultaneously to laboratory pressures, temperatures and stress over varying time spans. The experiments showed that track fading is a complex recovery mechanism, which is extremely sensitive to the coupling of these three parameters. In particular, a strong decrease in the fission track fading rate was observed as a function of increasing pressure. And a nearly temperature-independent dramatic increase in fission track recovery was observed as a function of stress. Consequently, (1) the stability field of fission tracks in apatite increases towards temperatures higher than 110°C depending on the absolute pressure; (2) closure ages in apatite are underestimated ($>100\%$ for an ideal geothermobarometric gradient); (3) related exhumation and erosion rates are overestimated above the closure temperature and underestimated below the closure temperature; and (4) since the widely applied statistical description of thermally induced fading kinetics does not account for the influences of either pressure or stress and is based on fission track annealing data produced at ambient pressure, the accuracy in extrapolating fission track data to geological time scales and in their application to dynamical systems must be cast into doubt.

* Corresponding author. Present address: British Antarctic Survey, Geosciences Division, Madingley Road, High Cross, Cambridge CB3 0ET, United Kingdom. Tel.: +44-1223-221-582; Fax: +44-1223-221-646.

E-mail addresses: aswe@bas.ac.uk (A.S. Wendt), olivier.vidal@ujf-grenoble.fr (O. Vidal), lewis.chadderton@anu.edu.au (L.T. Chadderton).

[1] Present address: LGCA, Université J. Fourier, 1381 rue de la Piscine, 38041 Grenoble, France.

0012-821X/02/$ – see front matter
PII: S0012-821X(02)00727-6

Keywords: fission tracks; apatite; annealing; temperature; pressure; stress; geochronology

1. Introduction

The constant and known rates of radioactive nuclear decay mean that the age of a mineral can be determined from ratios of the concentrations of parent to daughter elements. In track dating there is direct optical counting of chemically etched fission fragment tracks. Prior to etching latent tracks are generally complex linear trails of radiation damage which may be intermittent, lying on fragment trajectories, and consisting of point and extended defects, and/or new phases (e.g. amorphous material) in which a fragment's dissipated kinetic energy is stored [1–4].

Concerns about dating methods in general come from such factors as the possible gain or loss of the daughter element at some point in the history of the mineral (e.g. stability of the daughter product with respect to the geological environment). Other important factors include chemical composition and stoichiometry, crystal structure, and detailed technical mineral specifications [5–7,8–10]. By far the most important experimentally verified influential factor for the case of fission tracks from ^{238}U, however, has been temperature, and this especially for minerals used most commonly in geological applications. The general concept of a closure temperature – a specific temperature below which a daughter product (or track length) becomes 'frozen' in a crystal – was adopted for many radiometric systems [11]. Yet despite the recognition of temperature as a crucial parameter other potentially influential important physical parameters (e.g. pressure and stress) were taken to be negligible. The fact that the basic theory of atomic diffusion requires there to be an exponential decrease in the intrinsic diffusion coefficient with increasing pressure [8,12] was ignored.

In materials science, experiments on self diffusion in metals were conducted before the beginning of the 1970s, confirming basic theoretical concepts for lead [13,14] and zinc [15]. Unclear results for other metals (e.g. silver and uranium [16]) were attributed to their polycrystalline character. Diffusion in the alkali and noble metals [17] seemed to be independent of pressure. In the late 1960s and the 1970s, the annealing of fission tracks in minerals and glass (e.g. zircon and tectite [18,19]) at that time poorly understood as a complicated diffusion-enhanced process, was qualitatively investigated under pressure and stress. The results again indicated that temperature was the main driving force for fission track annealing. This early work was followed, e.g., by the description of a minor pressure dependence of argon diffusion in phlogopite [20], and more recently a non-linear pressure dependency of the diffusion of argon was discovered in rhyolitic glasses/melts [21]. Moreover, diffusional mechanisms under pressure were constrained in order to define the closure temperature of geothermometers based on Fe–Mg exchanges in olivine [22]. However, no systematic investigation of the influence of pressure and stress on diffusional mechanisms and recovery-rates in minerals relevant to geological dating systems has yet been reported.

This clear absence of reliable data on the pressure and stress dependencies of basic recovery processes governing those dating systems which involve crystalline annealing, or which are based on gaseous daughter products, prompted us to establish an experimental program for the quantitative study of the annealing systematics of fission tracks in minerals. We describe here results obtained for fission track annealing in apatite – one of the most commonly used minerals in geochronology – under pressure, temperature and stress.

Spontaneous fission tracks are nearly exclusively formed by the natural decay of ^{238}U present in crystalline or amorphous structures. When the tracks form, they are oriented randomly in space. Age determinations are based on a two-dimensional sampling of tracks intersecting an internal surface of the material, (e.g. by determining the density of fission tracks per cm^2 compared to the absolute amount of ^{238}U in the crystal). The probability of a shortened track intersecting a randomly selected surface is lower than the probabil-

ity of a long track intersecting the same surface. Thus, since the fission track age is determined by counting the number of tracks intersecting a surface, an older age is expected for a sample with longer tracks [5]. Based on this straightforward relationship of track density with track length, many experimental determinations of track stability were carried out over the past 20 years. A major purpose of studies of the evolution of track lengths as a function primarily of temperature and, secondarily, of time, was of course the development of realistic models leading to reliable extrapolation of the laboratory-derived length evolution data to geological time spans [23–26].

Here we measured the lengths and the density of etched spontaneous fission tracks in several apatite specimens, of different provenance and of different chemical composition. The samples were subjected (1) to various pressures P at constant temperature T and (2) to various temperatures and evolving compressional stress σ at constant pressure. In any of the P–T experiments, only one parameter was systematically changed in order to isolate the effect of each variable. Morphologically, no differences were observed between naturally annealed fission tracks and those fission tracks annealed under P, T and σ (Figs. 1 and 7), so that fission track analyses were performed using standard procedures.

We preferred, for two reasons, to investigate the annealing behavior of spontaneous tracks instead of using induced tracks as usually measured for most experimental T annealing studies [5,9,10,25,26]. The calculation for an exhumation path plus the calculation of exhumation and erosions rates are based on the analyses of spontaneous tracks in natural samples. This in turn might well introduce errors due to differences in the nature of the activated defects in induced and spontaneous tracks and their corresponding mobilities and lifetimes. Additionally, it is very probable that the self-annealing of freshly induced tracks is more active before final trapping of the defects than it is the case for ancient spontaneous tracks. Experiments on induced tracks might therefore not reflect the 'true' annealing behavior of spontaneous tracks. We are currently performing a series of P–T experiments on induced tracks in order to quantify the basic differences in their annealing behavior compared to the annealing of spontaneous tracks.

2. Experimental materials: description and preparation

Four types of apatite single crystals (length $\approx$30 mm, diameter $\approx$15 mm) of different composition were used for the experiments: a dark blue apatite from Siberia (Sludjanka), a light blue apatite from Canada, a dark green apatite from Madagascar and a light yellow–green apatite from Mexico (Durango). The relative fluorine/chlorine composition of the samples varied as follows: Siberia – 1:0.29, Canada – 1:0.08, Mexico – 1:0.27, Madagascar – 1:0.12. The mean initial FT length in all four types of apatite and the initial fission track densities for the apatites from Siberia and Canada are shown in Tables 1 and 2, respectively. The measurements were performed on sections parallel to the c-axis of the crystals.

The samples were cut and/or drilled parallel to their crystallographic c-axis and sealed into an annealed metal jacket (Au, Cu) before being placed into either the annealing or the deformation apparatus. Each apparatus operated with a different confining medium so that chemical interaction with the sample during the experiments had to be eliminated by removing 200 μm of the outer surface of the crystals after the experiment and before the fission track analysis. The pressurized samples were 5–10 mm in length and 4 mm in diameter. The deformed samples were 20 mm in length and 10 mm in diameter.

3. Experimental arrangement

Nearly 50 successful experiments were performed in studying the following P–T couplings: (1) 0.1 MPa, 250°C; (2) 0.1 MPa, 500°C; (3) 100 MPa, 250°C; (4) 200 MPa, 250°C; (5) 300 MPa, 250°C; (6) 600 MPa, 500°C; (7) 800 MPa, 500°C; and (8) 2000 MPa, 500°C. The experimental run times were fixed individually between 17 and 2200 h (Table 1). Depending on the experimental con-

ditions, different apparatuses (furnaces, externally heated pressure vessels, internally heated pressures vessels, solid-medium apparatus, Heard rig) were used in the Laboratoire de Tectonophysique in Montpellier, in the Laboratoire de Géologie of the Ecole Normale Supérieure in Paris, and in the Rock Deformation Laboratory, Department of Earth Sciences, University of Manchester. In all experiments, pressure and temperature were allowed to rise simultaneously to the desired P–T conditions, avoiding pre-test annealing.

1. Simple heating experiments at ambient pressure were performed in a furnace. The crystal slices were contained in a platinum crucible and were exposed to the atmosphere during the experiment. The cumulative uncertainty on the temperature measured with a Pt/13%Rhd thermocouple was ±5°C. The heating rate was equal to 5°C/min. Cooling to ambient temperature at the end of each run was achieved in 5 min. For each sample, only two ambient pressure runs were performed (168 h, 504 h) allowing a reasonable comparison of the observed fading behavior and the theoretically fading behavior predicted by the statistical approach of Laslett et al. [5].
2. Experiments at 100 and 300 MPa water pressure were performed in horizontal externally heated cold seal pressure vessels. The crystal slices were sealed in 2 cm long, 3 mm diameter gold capsules together with 2 ml distilled water. The confining pressure was controlled with a Bourdon gauge within ±0.3 MPa. The pressure was increased to half of the desired final pressure before heating. The temperatures were measured with a chromel–alumel thermocouple located at the hot end of the vessel and controlled within a precision of ±5°C. The heating rate was equal to about 20°C/min and the temperature overshoot above the desired temperature was less than 10°C in less than 10 min. At the end of each run, quenching of the capsules from 500°C to ambient temperature was achieved in 10 min before decompression.
3. The high pressure runs at 600 and 800 MPa were performed in an internally heated pressure vessel. The confining pressures were built up with argon gas and electronically controlled within ±1 MPa. The cumulative uncertainty on temperature measured with Pt/13%Rhd thermocouples located at both ends of the pressure chamber was measured and controlled within ±3°C of precision. The T-gradient in the pressure chamber was measured electronically and was less than 1°C. The experimental heating rate was equivalent to 20°C/min. Cooling to ambient temperature at the end of the experiments was achieved in 1 min before decompression.
4. The ultra-high pressure runs at 2000 MPa were performed in a solid-medium apparatus in which the confining pressure was achieved by flowing salt. The experimental heating rate was equivalent to 15°C. The cumulative uncertainties in temperature measured with Pt/13%Rhd were electronically controlled within ±2°C. Cooling to ambient temperature was achieved under pressure in about 90 min.
5. Triaxial compressional deformation experiments were conducted with a Heard rig at a confining pressure of 280 MPa corresponding to the maximum applicable pressure for this apparatus, temperatures were of 20 and 250°C. Electronically controlled loading rates were 10^{-5} mm/s and 10^{-7} mm/s, respectively. Pressure was controlled in the range of ±15 MPa and temperatures with a Pt/13%Rhd thermocouple were electronically controlled within ±5°C of precision. Cooling to ambient temperature was achieved at zero load under stepwise pressure release in about 120 min.

4. Sample preparation after treatment

The samples were sometimes broken after the experiments due to decompression, but did not change color. Both initial and final apatites (e.g. run products) were embedded in epoxy resin and ground on 1000 mesh SiC papers to expose internal crystal surfaces. These were then polished on a Struers Rotopol-22 apparatus equipped with a Rotoforce-4 sample holder, using 3 and 1/4 μm

diamond pastes. Approximately 200 μm of material were removed from the crystal surface in order to avoid blurring of the experimental results by interactions between the confining media (air, water, argon, oil) and the crystal. All samples were etched in a bath of $HNO_3:H_2O = 5$ mol/1000 ml, magnetically stirred, at room temperature for 20 s, then rinsed in distilled water to arrest the etching. They were then washed first in water, and afterwards with alcohol [5,6,24]. Fission track analyses were exclusively performed on confined spontaneous tracks of the track in track type (TINT) in crystal planes parallel to the crystallographic *c*-axis of the minerals.

After etching, the lengths and orientation of horizontally confined tracks of the TINT (in average 117 points/sample) and fission track densities per cm^2 (average number of counted tracks per sample: 5000) were measured with an optical microscope (ZEISS Axioplan 2) at a true magnification of 1250. For performing length measurements, the microscope was equipped with a drawing tube that projected a point-like light source mounted on the cursor of a Calcomp Drawingboard digitizer (CalComp, CSP), positioned next to the microscope, onto the microscope image. Regular control measurements were performed using a true magnification of 2500. The error between the two types of measurements was, on the average lower than 0.02 μm. The coordinates of the track extremities, indicated with the cursor, were sent on-line to a MacIntosh computer, and read in the Trevorscan FT-stage program, which calculated and stored the confined track lengths and orientations. The direction of the *c*-axis of the apatite crystals was entered as the reference orientations.

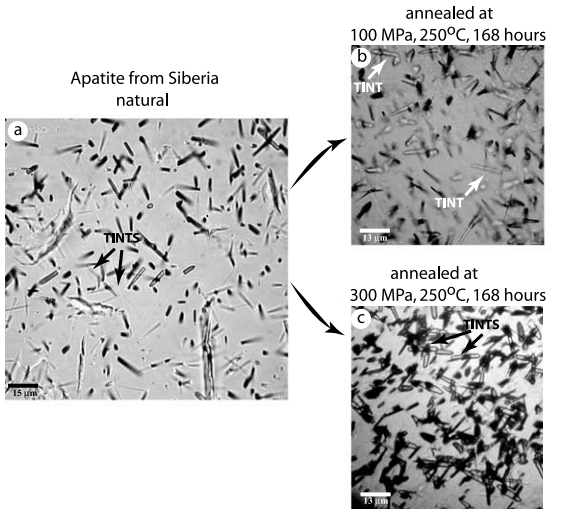

Fig. 1. Natural, *T*-annealed and *P–T*-annealed fission tracks. Optical photomicrographs taken in transmitted light of fission tracks in a Siberian apatite. (a) The original spontaneous fission tracks, (b) spontaneous fission tracks in the same crystal after annealing for 168 h at 100 MPa and 250°C and (c) spontaneous fission tracks in the same crystal after annealing for 168 h at 300 MPa and 250°C. The photomicrographs (b) and (c) were taken using an oil immersion objective lens.

All measurements were performed by the same analyst (A.S.W.) and regular control measurements were performed by measuring track lengths and densities twice on the same sample. Length

Table 1
Quantitative measure of annealing: change in length of horizontally confined fission tracks under *P* and *t* at $T = 250$°C compared to the initial lengths

Sample	Number of measured lengths	Initial mean length	Mean length at 0.1 MPa		Mean length at 100 MPa			Mean length at 200 MPa	Mean length at 300 MPa		
		(μm)	(μm)		(μm)			(μm)	(μm)		
			168 h	504 h	168 h	504 h	2200 h	17 h	168 h	504 h	2200 h
Madagascar	>110	13.24	12.21	11.39	12.85	12.71	11.27	13.21	13.17	13.02	11.76
Canada	>110	13.64	11.60	9.50	12.68	12.43	11.05	13.60	13.31	13.01	11.62
Siberia	>110	13.68	11.51	9.25	12.51	12.26	10.95	13.32	12.91	12.67	11.22
Mexico	50	14.21	11.40	9.30	12.48	12.15	10.75	13.69	13.09	12.74	11.40

Measurements of confined mean track lengths in the initial samples and the *P–T*-annealed samples at a constant temperature of 250°C.

measurement and density uncertainties were below 1% for all run-products from the samples from Canada, Siberia and Madagascar due to the statistically sufficient number (>100 for length, 5000 counts per sample) of measured tracks. The uncertainties for the sample from Mexico were only lower than 5% due to the relatively small number of tracks in the sample.

In cases where insufficient horizontally confined fission tracks were found, the samples were irradiated with fragments from a Californium source allowing deeper etching. The Californium irradiation was performed by R. Donelick, Donelick Analytical, Inc., using a ^{252}Cf source (U.S. Geological Survey). During irradiation, the samples were centered under an Isotope Products Laboratories 50 μCi ^{252}Cf source (FF-252-4) at a distance of 8.2 cm below the active surface. Then, the irradiation apparatus including the ^{252}Cf source and the specimens were placed under a near vacuum (<666 Pa) for a total period of 68 h 5 min. Following irradiation, etching and measurements were performed as described above.

Confined track lengths were measured in all run-products to allow a quantitative comparison of the fading behavior for the four apatite compositions. Track density measurements, only allowing a qualitative comparison of the fading behavior due to inhomogeneous distribution of ^{238}U throughout the crystals, were restricted to some runs-products from only two specimens.

5. Experimental results

Fig. 1 shows two optical photomicrographs of

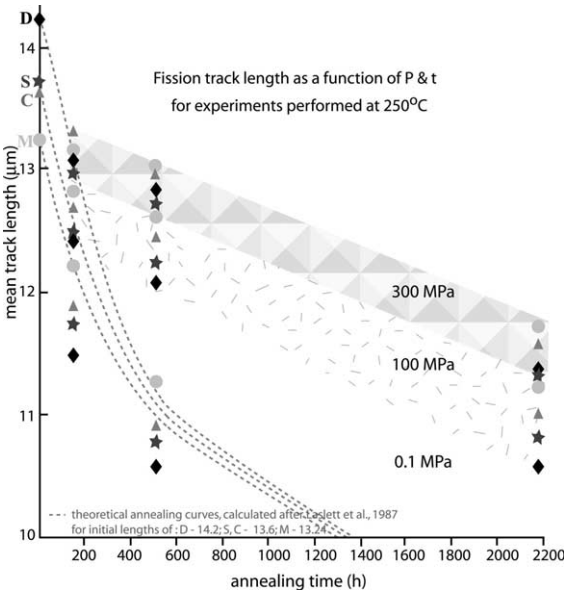

Fig. 2. Mean length evolution of *P–T*-annealed fission tracks. Length evolution of ^{238}U fission tracks at different confining pressures. Fluorine/chlorine sample composition: D – 1:0.27; S – 1:0.29; C – 1:0.08; M – 1:0.12. Pressure and temperature values were corrected for measurement uncertainties. Length uncertainties are greatest for D-sample due to the limited number of horizontally confined ^{238}U fission tracks. D – Durango apatite (Mexico); S – Siberia-apatite; C – Canada apatite; M – Madagascar apatite. (Calculated) equivalent times used for theoretical curves: D – 5 h; S,C – 17 h; M – 35 h.

pressure-annealed fission tracks compared to the unannealed sample. Morphologically, no differences could be observed between the naturally annealed sample, the *T*-, the *P–T*-, and the *P–T–σ*-annealed samples, so that in all cases, fission track analyses were performed using the standard procedure already described.

Table 2
Qualitative measure of annealing: change in density of fission tracks under *P* and *t* at *T*=250°C compared to the initial densities

Sample	Number of counts	Initial ρ	ρ at 0.1 MPa	ρ at 100 MPa		ρ at 300 MPa	
		(FT/cm^2)	(FT/cm^2)	(FT/cm^2)		(FT/cm^2)	
			168 h	168 h	504 h	168 h	504 h
Canada	5000	25711 98	1866957	2108382	2031246	2344933	2275000
Siberia	5000	2726208	1790455	2126442	1990132	2397241	2326742

Measurements of densities in the apatites from Siberia and Canada before and after *P–T* annealing at 250°C. The maximum variation in the distribution of ^{238}U was determined to be lower than 20%.

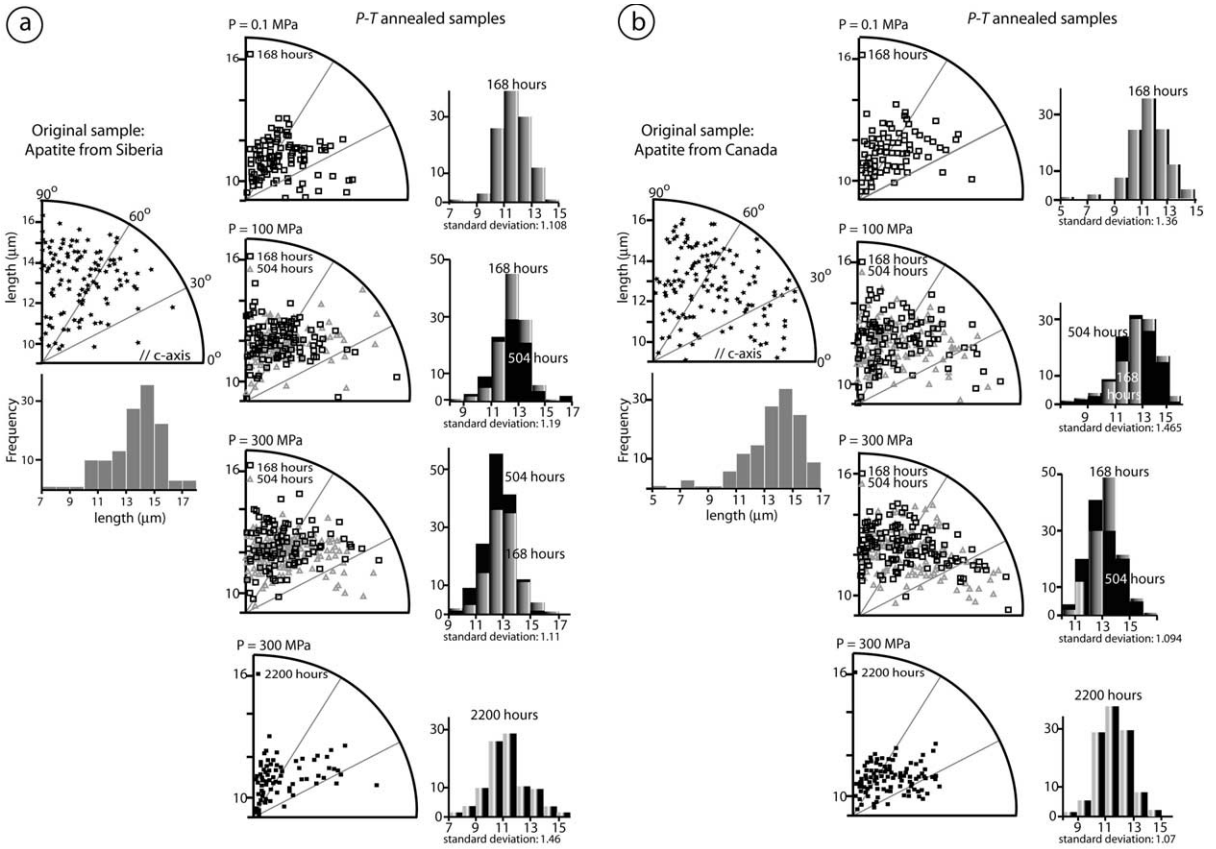

Fig. 3. (a,b) Polar plots and frequency distribution of fission track lengths. The orientation to the crystallographic *c*-axis of the samples and the length distribution of horizontally confined spontaneous tracks are shown for some apatite run-products. All samples were annealed at a temperature of 250°C, various pressures (as indicated) and time spans of 168–2200 h (as indicated).

5.1. *P annealing experiments at 250°C*

The pressure experiments permitted definition of the changes in the confined mean track length as a function of confining pressure and crystal composition at a constant temperature of 250°C. These results are summarized in Fig. 2. The initial track length (as measured) in all four apatite specimens appears on the *y*-axis at time zero. The lengths after *P–T* annealing are then displayed as a function of the experimental run time. The absolute measurements of length are given in Table 1.

The fading rate as observed from the length measurements decreased considerably with increasing pressure. After an experimental run time of 2200 h, fission tracks are in average 2 µm longer (average length: 11 µm) at 100 MPa pressure and in average 2.5 µm longer (average length 11.5 µm) at 300 MPa compared to the theoretically predicted length (calculated using equation 14 in [5]) of approximately 9.0 µm at 0.1 MPa.

However, despite the average increase of the FT stability with increasing confining pressure, fission tracks fading seems to follow a specific annealing rate for any individual crystal. This might be due to differences in composition (e.g. impurities). It can be observed in Fig. 2, that the chlorine-poor sample from Canada has a slower annealing rate than the chlorine-richer sample from Siberia, despite both specimens displaying a similar initial mean track length. It can be also observed that shorter initial tracks (sample

from Madagascar) have a slower annealing rate than longer tracks in an apatite of similar chemical composition (sample from Mexico).

Some examples of the length distributions for horizontally confined spontaneous tracks are presented in polar plots and their frequency distributions are given in histograms in Figs. 3a,b. The initial length distributions were basically unimodal though with a very small component of short tracks (<9 μm) for the apatite from Siberia. The apatite from Canada showed a more complex track distribution with a unimodal core-distribution containing most of the tracks and a distinct population of tracks with short lengths (<9 μm). The standard deviation of the frequency length distribution was for both initial samples in average 1.80 and the standard error was 0.14. During *P–T* annealing the mean track length decreased in all run products. Tracks oriented parallel to the *c*-axis of the crystal shortened slightly faster, so that the maximum number of tracks was sampled at 45–90° to the *c*-axis of the specimens. This effect was slightly stronger for the apatite from Siberia. The more complex track distribution in the sample from Canada was reduced to a more narrow unimodal distribution after a run time of 2200 h at a confining pressure of 300 MPa (Figs. 3a,b). This basically signifies that longer tracks oriented parallel to the *c*-axis of the sample shortened faster than the tracks of medium length, and that already short tracks shortened below their optical limit of detection. This observation – anisotropic annealing as a function of the initial length during

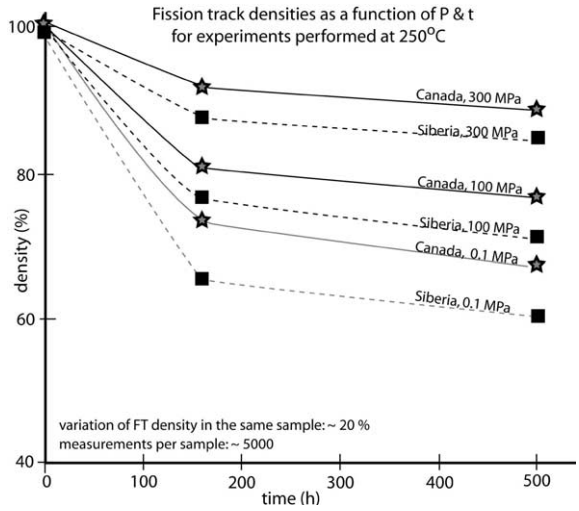

Fig. 4. Changes in fission track density. Experimental results on changes in the fission track density after annealing at different pressures (*P*) (0.1, 100, 300 MPa) and constant temperature (*T*, 250°C) for two different time spans (168 h, 504 h). Initial fission track densities (100%) appear on the *y*-axis at time zero.

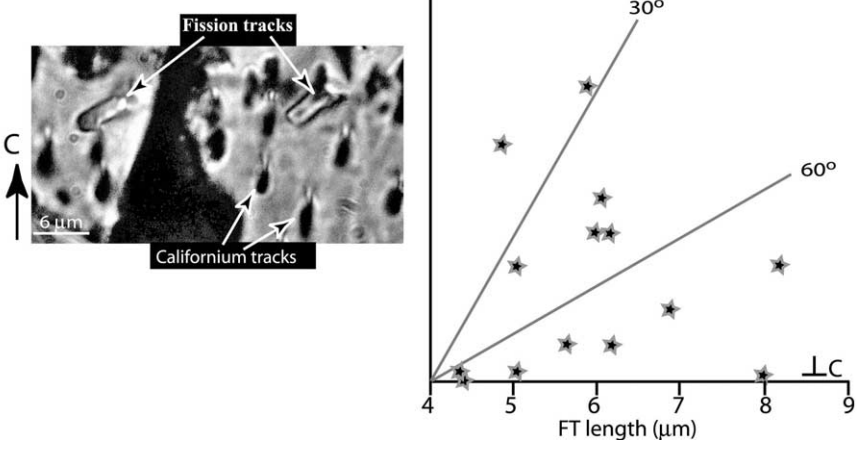

Fig. 5. Annealing results at ultra-high *P* and high *T*. Fission tracks were annealed for 168 h at a 2000 MPa confining pressure and at 500°C. The fission track distribution reveals (as anticipated) a maximum number of fission tracks at a greater angle to the *c*-axis of the sample. The optical photomicrograph was taken using an oil immersion objective lens.

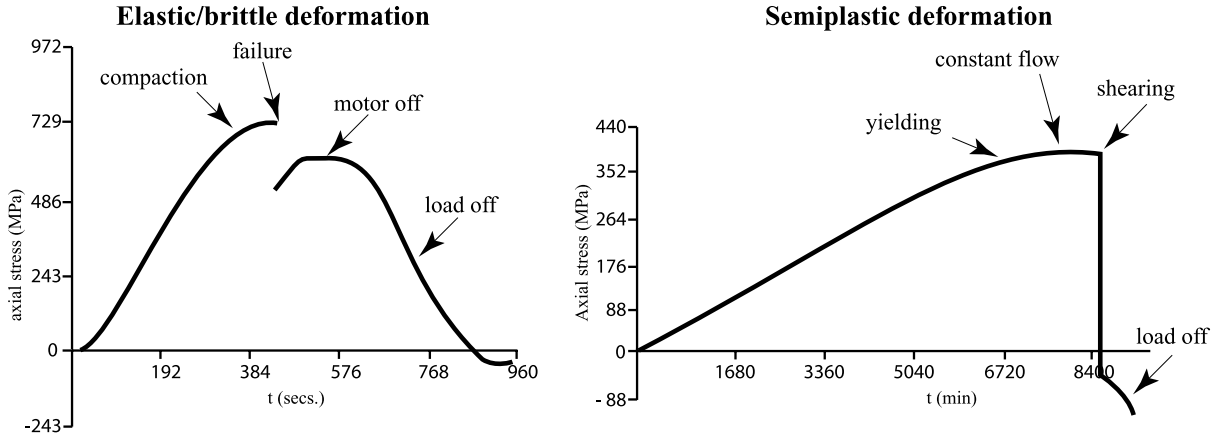

Fig. 6. Triaxial deformation experiment. Evolution of compressional stress during experimental run-time. The loading rate during elastic/brittle deformation was 10^{-5} mm s^{-1} and, during semi-plastic deformation 10^{-7} mm s^{-1}.

P–T-depending recovery – confirmed earlier observations made during *T*-depending annealing experiments [10].

Changes in the FT density are shown for two apatite compositions (Canada, Siberia) as a function of pressure, temperature and time in Fig. 4. They are represented in simple cartesian coordinates as a function of time. The initial percentage track densities for both crystals appear on the *y*-axis at time zero. The track densities after annealing are then shown as being dependent on the annealing time and the applied pressure, absolute values being given in Table 2. Inhomogeneities in the ^{238}U distribution were determined to be lower than 20% in the two apatites by measuring FT density variations throughout the total polished surface of each run-product. For both apatite crystals, the increase of pressure at constant temperature led to a better preservation of the fission tracks compared to annealing at ambient pressure, and thus confirmed qualitatively the observation made on the evolution of confined fission track lengths.

5.2. *P* annealing experiments at 500°C

Experiments performed at 500°C were only successful at 2000 MPa, in which, after a duration of 168 h, fission tracks with a mean length minimum of 6.3 μm were still remaining (Fig. 5). Note that due to the limited number of detected tracks, not all measured tracks were horizontally confined, which in turn biased the absolute mean length values. At lower pressures for the same temper-

Table 3
Quantitative measure of annealing: change in length of horizontally confined fission tracks under *P* and *t* at *T* = 500°C compared to the initial lengths

Sample	Initial mean length (μm)	Number of measured lengths	Mean length at 0.1 MPa (μm)	Mean length at 600 and 800 MPa	Mean length at 2000 MPa
			5 h	168 h	168 h
Madagascar	13.24	0	no tracks	no tracks	no experiment
Canada	13.64	14	no tracks	no tracks	6.3
Siberia	13.68	0	no tracks	no tracks	no experiment
Mexico	14.21	0	no tracks	no tracks	no experiment

Measurements of confined mean track lengths in the initial samples and the *P–T*-annealed samples at a constant temperature of 500°C.

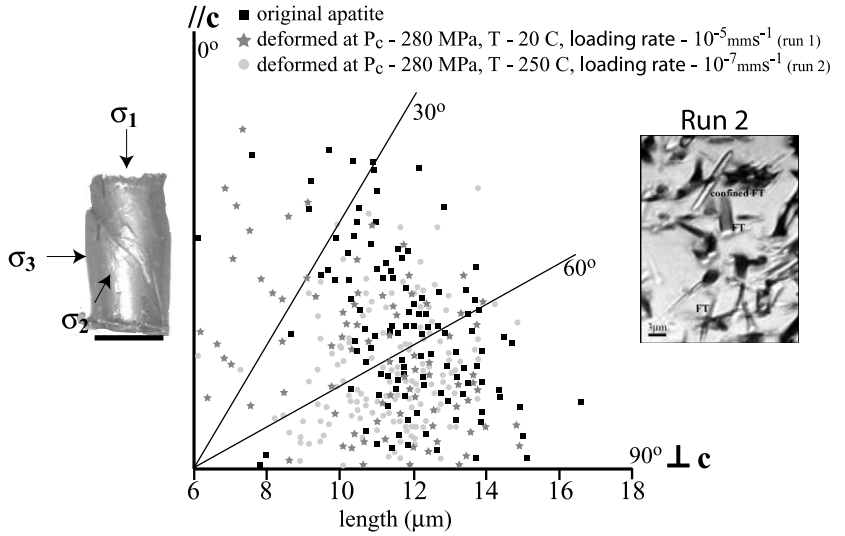

Fig. 7. Crystallographically controlled annealing of fission tracks. Plot of length evolution of ^{238}U fission tracks relative to the crystallographic *c*-axis of apatite (Madagascar sample) in compressional deformation regimes. The mean track length changed during run 1 to 12.28 µm and during run 2 to 12.03 µm. $\sigma_1 > \sigma_2 = \sigma_3$ (σ-stress). Small cylinder: sample after 1 week of compressional deformation at 250°C. Optical photomicrograph taken in transmitted light using an oil immersion objective.

ature, fission tracks had annealed in all experiments below the etchable, and thus optically detectable length. In fact, they anneal below detectability in only 5 h at ambient pressure (0.1 MPa) and 500°C (Table 3).

These high temperature experiments, then, confirmed again that increasing pressure decreases the annealing kinetics of fission tracks in apatite, and that the fading rate is sensitive to the *P–T* coupling.

5.3. σ annealing experiments at 280 MPa and 250°C

The deformation experiments allowed us to investigate the annealing behavior of spontaneous fission tracks under elastic/brittle and semi-plastic conditions. The first sample was elastically deformed at a confining pressure of 280 MPa, a temperature of 20°C and a loading rate of 10^{-5} mm/s until it broke. The total duration of the experiment was 16 min and the maximum compressional stress reached 730 MPa for a total axial deformation of 20.80%. Semi-plastic deformation was conducted on the second sample at a confining pressure of 280 MPa, a temperature of 250°C and a loading rate of 10^{-7} mm/s until nearly constant flow stress develop before shearing at 45° to the maximum stress direction occurred. Here, the total run time was 8400 min and the maximum compressional stress reached 421 MPa for a total axial deformation of 11.90% (Fig. 6).

Despite the absence of optically detectable, morphological differences (Figs. 1 and 7) between *T*-annealed, *P–T*-annealed and *P–T–σ*-annealed fission tracks (no broken tracks, hardly any tracks with unetchable gaps) were not observed, the changes in the mean track length during both deformation experiments were dramatic compared to the *T*- and *P–T*-annealing experiments. The mean track length decreased during elastic/brittle deformation from 13.24 to 12.28 µm in only 16 min total run time and during semi-plastic deformation from 13.24 to 12.03 µm in 140 h (Table 4). During the corresponding *P–T* experiment, the mean fission track length remained at 12.70 µm after an experimental run time of 168 h (Fig. 7). Thus, both differential elastic/brittle stress and differential semi-plastic stress appeared to enhance fission track annealing nearly independent of the applied temperature. Additionally, the semi-plastic deformation (performed at *T*) in-

duced crystallographically preferred annealing preserving tracks oriented in the main in the angular interval between 40 and 90° to the crystallographic *c*-axis of the specimen (Fig. 7) which is in good agreement with the anisotropic annealing behavior observed during the earlier *T* experiments [10] and the *P–T* experiments from this work.

Summarizing, we can say that the experimental results presented here, indicate (1) that the annealing rate of spontaneous fission tracks in apatite decreases with confining pressure for experimental time duration, (2) that differential stresses dramatically increase the annealing rate and induce an annealing anisotropy when coupled with temperature and (3) that each type of apatite has an individual activation volume (depending on chemical composition and/or initial mean track length) and that there is no one typical annealing behavior.

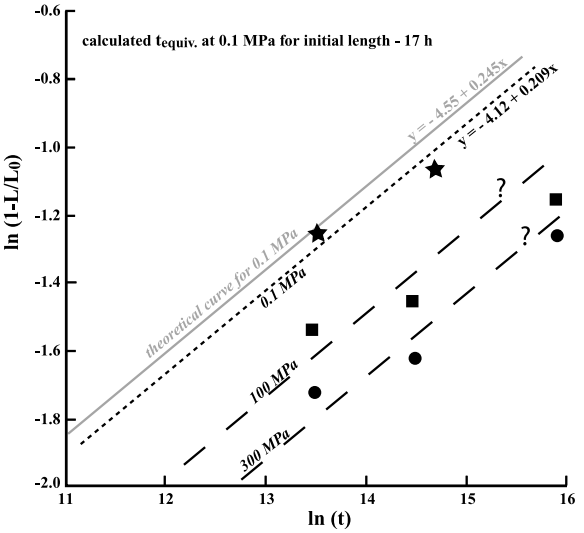

Fig. 8. Modelling fission track annealing. The statistical model describing fission track annealing of Laslett et al. [5] applied to the pressure runs for Canadian apatite. Comparisons are made between the measured and theoretically predicted values at ambient pressure. The curves were derived on the basis of equation 14 of Laslett et al. [5] calculated by least square regression with a constant slope ($B = 0.245$, derived from the theoretical curve). Changes with pressure of the kinetics of annealing due to variations of the activation energy ($R \times C = E + P \times V$) where E (1 bar) is the activation energy, P is the experimental pressure and V is the activation volume.

6. Discussion

Pressure experiments similar to those described here were earlier conducted on crystals of zircon [27]. In these experiments, pressure-dependent annealing was not observed and the resulting recovery behavior was similar to annealing at atmospheric pressure [28]. This observation on zircon, together with our results for apatites of different compositions, seems to establish experimentally that fission track recovery kinetics are dependent upon the specific material properties of each type of mineral (heated, pressured or stressed), which correlates well with the other observations on the complicated pressure dependence of diffusion in metals and other minerals [13–17,27,28].

The removal of latent fission fragment tracks in crystals is of course the inverse phenomenon in physics of primary registration. It has been customary to consider track formation in terms of conversion of the energy deposited into lattice heat. This essential thermal spike [29], in which only macroscopic target properties and track widths are concerned, no system cooling is allowed for, and no rapid 'in situ' recovery processes are permitted [30], often fails dismally. We cite the example of a complete absence of fission tracks in graphite and silicon, which amorphize

Table 4
Quantitative measure of annealing: change in length of horizontally confined fission tracks under P and σ at $T = 250$°C

Sample	Initial mean length (μm)	Number of measured lengths	Mean length at 280 MPa (μm)	
			loading rate = 10^{-5} mm s^{-1}	loading rate = 10^{-7} mm s^{-1}
Madagascar	13.24	> 110	12.28	12.03

Change in mean lengths of ± confined tracks under compressional triaxial deformation.

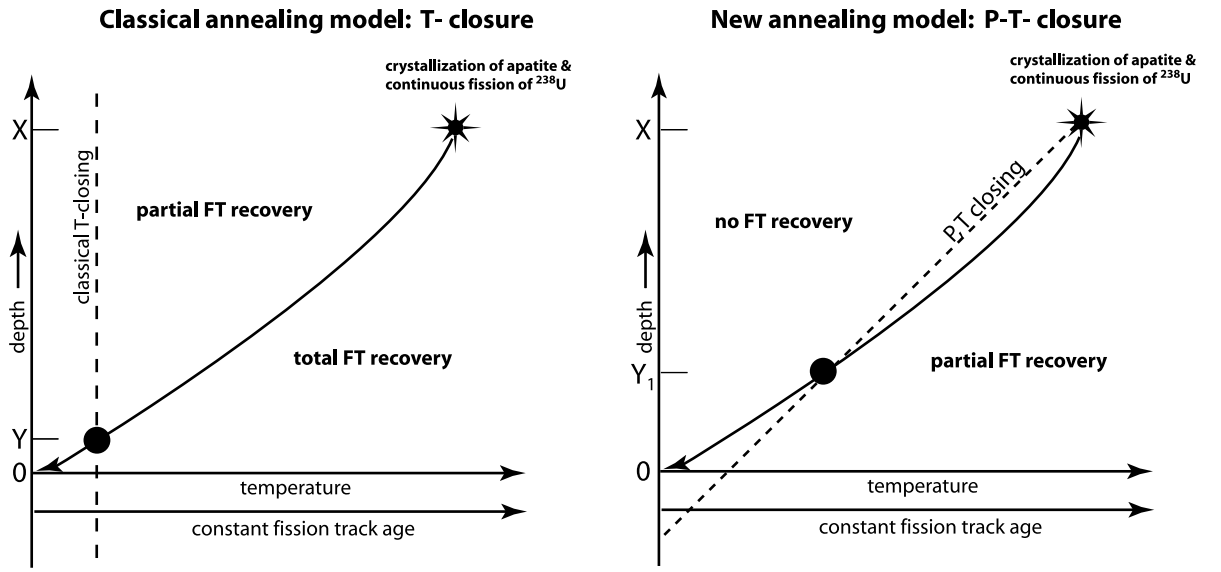

Fig. 9. Geological consequences. Comparison between T and P–T annealing of ^{238}U fission tracks and a qualitative estimate of the error introduced to closure temperature/age, exhumation and erosion rates. The classical closure temperature (cT) for fission track annealing (below which the annealing becomes equivalent to zero) in apatite is around 100°C (e.g. [6]). The cT is attributed to the fission track age of the apatite – that is a constant, calculated from the ratio between parent and daughter product (age of reaching the cT = closure age). Consequently, a higher cT (due to the effect of pressure) corresponds to a greater depth at a given constant fission track age. This leads to an overestimation of the exhumation and erosion rates below, and an underestimation of exhumation and erosion rates above the pressure dependent cT (compared distances between depth $X-Y$ and $Y-0$ in the classical model and $X-Y_1$ and $Y-0$ in the new model).

readily and where tracks should therefore form. In each case the answer lies with defects specific to the target – the three-dimensional divacancy in diamond cubic silicon and the two-dimension divacancy in hexagonal graphite [31]. Rapid creation and very swift motion means that these specific defects catalyze total epitaxial crystal recovery from the random (amorphous), or only partially crystalline transient track virtually immediately it is formed (10^{-12} s). This 'projectile-assisted prompt anneal' is an entirely new approach to track registration based on the behavior of identified and crystal characteristic 'point' defects, and is the short-term equivalent of 'defect activated delayed anneal' [32] which we studied here. As a complying example of only partial epitaxial recovery we cite the case of intermittent track structure in fluorite (CaF_2), which is due to fluorine crowdion interstitial (V_h centers) on the anion sublattice [3,31,32].

Apatite, like muscovite mica, is a 'well-behaved' geochronological mineral in terms of both fission track registration and annealing and recovery, and in what is almost certainly local epitaxial recovery [33]. Whilst we have not yet identified the 'point' defects responsible for track registration and recovery in apatite it is clear from the results that we have described, that pressure will have a confining effect – reducing the defect jump frequency responsible for diffusion (an increase in the height of the activation barrier) – and retarding recovery [34]. Similar defect motion must be preferentially expected down stress and/or pressure gradients.

The different annealing rates that we observe for different apatites are perfectly in accord with either different characteristic responsible defects, or an intrinsic association with a variety, and variable concentration of 'impurity' defects. Impurity atoms, single or in clusters are, in chemical kinetics, unsaturable traps for mobile defects [35].

In light of these considerations, the results presented suggest that temperature can no longer be considered as the only important parameter influ-

encing track recovery. Annealing needs to be considered for what it is: a complex interplay of diffusional mechanisms, material properties (e.g. the specific defect characteristics) and the full range of physical parameters in the (natural) environment. This complexity needs to be included in any mathematical model aimed at describing track recovery. The widely applied statistical model describing track annealing in apatite [5] cannot reproduce the pressure- and stress-derived length evolution (Fig. 8), and is therefore only valid for describing apatite-recovery kinetics in those geological contexts where both factors play a minor role.

In the more general case, in which both pressure and temperature are part of the natural environment, the fission track annealing models available in the literature must be rearranged to account for the experimentally shown P and T dependency of the diffusion coefficient with

$$D = D_0 \exp\left[(-Q - PV)/kT\right] \quad (1)$$

where D_0 is the diffusion coefficient at ambient temperature and pressure, Q the activation energy at 0.1 MPa, V the activation volume, k the Boltzmann's constant.

Then, for example, the constant B in the parallel Arrhenius model of Laslett et al., ([5] equation 14)

$$\ln\left[1-(L/L_0)\right] = \ln(t) - BT^{-1} \quad (2)$$

with L_0 is the initial track length, L the final track length, and t is the time, can be rearranged so that

$$B = -(Q + PV)/k \quad (3)$$

However, if the results of the above laboratory experiments are extrapolated to relevant 'geological' time durations, we may anticipate that the commonly accepted closure temperature for FT annealing (e.g. the temperature at which the rate of annealing tends to zero; about 100°C at 0.1 MPa) as well as the 'partial annealing zone' (60–110°C at 0.1 MPa, [5]) will be higher in most natural conditions for which $P > 0.1$ MPa ($P \sim 100$ MPa at ~ 100°C) and prolong the recovery time by more than 100% for annealing during exhumation along an equilibrated geothermobarometric gradient.

The implications of these results for the application of geological dating methods as well as for related geodynamics interpretations are both significant and intimidating. For the apatite fission track method alone, the results mean that since tracks are more stable under hydrostatic pressure, and since tracks in nature will be mostly exposed to P and T, the closure ages (temperature–age relationship) during exhumation will be strongly underestimated. Related exhumation paths will likely need complete revision whilst attributed exhumation/erosion rates may be totally overestimated below and underestimated above the P-closure temperature (Fig. 9). Major errors are to be expected for exhumation rates of pressure-dominated metamorphic regimes. Since tracks fade faster when subjected to differential stress, then, in this context, closure ages represent rather a (local) stress field than a P–T point.

It follows that future use of the apatite fission track method in its current state, seems to be justified only in those geological environments where temperature is the excess parameter compared to pressure and stress (e.g. contact metamorphism, rise of plutons, regions of high geothermal gradient). For all other applications, a new mathematical model – constrained by experimental data – is urgently needed. One which allows us to predict fission track annealing in a range of apatite (and other crystalline) compositions for various P–T($-\sigma$) conditions.

7. Conclusion

In this work, we have demonstrated that the annealing of fission tracks in apatite is extremely pressure and stress sensitive. In their present form applications of current annealing models to geological problems are limited and introduce significant errors in the derivation of closure ages, exhumation paths, and of exhumation and erosion rates. This in turn underlines the need for a deeper understanding of the basic physics of diffusion kinetics in geological applications generally, in-

cluding other geological dating systems (e.g. U–Th/He, [36]), deformation mechanisms (e.g. diffusion governed dislocation climb, superplasticity) and large-scale problems in the challenge of understanding thermal diffusivity in the upper mantle.

It has not escaped our notice that latent fission tracks created in apatite and other minerals under strong hydrostatic pressure may well also be both broadened and foreshortened in length at birth due to suppression of defect motion and mineral recovery. Similarly the well-known random computer simulations of fragment ranges, etc., are of little value if ambient pressure is present since persistent diffusion and real defect recovery processes are not accounted for.

Acknowledgements

We thank B. Goffé for providing the experimental apparatuses for performing experiments at pressure and temperature, and E. Rutter for providing the Heard rig to carry out experiments at pressure, temperature and stress. The supervision of the deformation experiments by R. Holloway is gratefully acknowledged. We also thank M. Brunel, F. Brunet, A. Carter, K. Gallagher, A. Hurford, R. Jonkheere, D. Mainprice, J.-F. Ritz and G. Wagner for interesting and extended discussions and technical support. We are also indebted to R. Jonckheere and O. Maurel for double-checking length and density measurements in some samples, and to E. Enkelmann and C. Nevado for the preparation of thin sections. Support from the Deutsche Forschungsgemeinschaft (Habilitation Fellowship We 1937/2-4) is gratefully acknowledged (A.S.W.). One of us (L.T.C.) acknowledges also support from CSIRO (Australia).*[BW]*

References

[1] L.T. Chadderton, J.P. Biersack, S.L. Koul, Discontinuous fission tracks in crystalline detectors, Nucl. Tracks Radiat. Meas. 15 (1988) 31–40.
[2] M. Toulemonde, Nanometric phase transformation of oxide materials under GeV energy heavy ion irradiation, Nucl. Inst. Methods Phys. Res. 156 (1999) 1–11.
[3] L.T. Chadderton, Track formation, Track 10 (2000) 5–8.
[4] L.T. Chadderton, I. M. Torrens, Fission Damage in Crystals, Methuen, London, 1969.
[5] G.M. Laslett, P.F. Green, I.R. Duddy, A.J.W. Gleadow, Thermal annealing of fission tracks in apatite. 2. A quantitative analysis, Chem. Geol. 65 (1987) 1–13.
[6] G.A. Wagner, P. Van den Haute, Fission Track Dating, Ferdinand Enke Verlag, Stuttgart, 1992, pp. 285.
[7] K. Gallagher, R. Brown, C. Johnson, Fission track analysis and its application to geological problems, Annu. Rev. Earth Planet. Sci. 26 (1998) 519–572.
[8] Y. Adda, J. Philibert, La diffusion dans les solides: Bibliothèque des Sciences et Techniques Nucléaires, Presses Universitaire de France, Paris, 1966, pp. 810–853.
[9] W.D. Carlson, R.A. Donelick, R. Ketcham, Variability of fission-track annealing kinetics: I. Experimental results, Am. Mineral. 84 (1999) 1213–1223.
[10] R.A. Donelick, R.A. Ketcham, W.D. Carlson, Variability of apatite fission-track annealing kinetics: II. Crystallographic orientation effects, Am. Mineral. 84 (1999) 1224–1234.
[11] M.H. Dobson, Closure temperature in cooling geochronological and petrological systems, Contrib. Min. Petrol. 40 (1973) 259–274.
[12] R.W. Keyes, Volume of activation, II. Pressure dependence of activation parameters, J. Chem. Phys. 32 (1960) 1066–1067.
[13] N.H. Nachtrieb, H.A. Resing, S.A. Rice, J. Chem. Phys. 23 (1955) 1193, in: Y. Adda, J. Philibert (Eds.), La diffusion dans les solides, Bibliothèque des Sciences et Techniques Nucléaires, Presses Universitaire de France, Paris 2, 1966, 831 pp.
[14] J.B. Hudson, R.E. Hoffman, Transactions AIME 221 (1961) 761, in: Y. Adda, J. Philibert (Eds.), La diffusion dans les solides, Bibliothèque des Sciences et Techniques Nucléaires, Presses Universitaire de France, Paris 2, 1966, 831 pp.
[15] T. Liu, H.G.J. Drickamer, Chem. Phys. 22 (1954) 312, in: Y. Adda, J. Philibert (Eds.), La diffusion dans les solides, Bibliothèque des Sciences et Techniques Nucléaires, Presses Universitaire de France, Paris 2, 1966, 831 pp.
[16] M. Beyerler, Y. Adda, Physics of Solids at high Pressures (1965) 349, in: Y. Adda, J. Philibert (Eds.), La diffusion dans les solides, Bibliothèque des Sciences et Techniques Nucléaires, Presses Universitaire de France, Paris 2, 1966, 831 pp.
[17] Y. Adda, J. Philibert, La diffusion dans les solides: Bibliothèque des Sciences et Techniques Nucléaires, Presses Universitaire de France, Paris, 1966, 827 pp.
[18] R.L. Fleischer, P.B. Price, R.M. Walker, Effects of temperature, pressure and ionization on the formation and stability of fission tracks in minerals and glasses, J. Geophys. Res. 70 (1965) 1497–1502.
[19] R.L. Fleischer, R.T. Woods Jr., H.R. Hart, P.B. Price, Effect of shock on fission track dating of apatite and

sphene crystals from the hardhat and sedan underground nuclear explosions, J. Geophys. Res. 79 (1974) 339–342.
[20] B.J. Gilletti, J. Tullis, Studies in diffusion, IV. Pressure dependence of Ar diffusion in phlogopite mica, Earth Planet. Sci. Lett. 35 (1977) 180–183.
[21] H. Behrends, Y. Zhang, Ar diffusion in hydrous silicic melts: implications for volatile diffusion mechanisms and fractionation, Earth Planet. Sci. Lett. 192 (2001) 363–376.
[22] O. Jaoul, Y. Bertran-Alvarez, R.C. Liebermann, G.D. Price, Fe–Mg interdiffusion in olivine up to 9 GPa at $T = 600$–900°C; experimental data and comparison with defect calculations, Phys. Earth Planet. Int. 89 (1995) 199–218.
[23] A.J.W. Gleadow, I.R. Duddy, P.F. Green, J.F. Lovering, Confined track lengths in apatite – a diagnostic tool for thermal history analysis, Contrib. Mineral. Petrol. 94 (1986) 405–415.
[24] P.F. Green, I.R. Duddy, A.J.W. Gleadow, P.R. Tingate, G.M. Laslett, Thermal annealing of fission tracks in apatite: 1. A qualitative description, Chem. Geol. 59 (1986) 237–253.
[25] W.D. Carlson, Mechanisms and kinetics of apatite fission-track annealing, Am. Mineral. 75 (1990) 1120–1139.
[26] K.D. Crowley, M. Cameron, R.L. Schaefer, Experimental studies of annealing of etched fission tracks in fluorapatite, Geochim. Cosmochim. Acta 55 (1991) 1449–1465.
[27] M.R. Brix, B. Stöckhert, E. Seidel, T. Theye, S.N. Thomson, M. Küster, Thermobarometric data from a fossil zircon partial annealing zone in high pressure-low temperature rocks of eastern and central Crete, Greece. Tectonophysics 349 (2002) 309–326.
[28] T. Tagami, R.F. Galbraith, R.F. Yamada, G.M. Laslett, in: P. Van den haute, F. De Corte (Eds.), Advances in Fission-Track Geochronology, Kluwer Akademic Publishers, Dordrecht, 1998, pp. 99–112.
[29] L.T. Chadderton, Radiation Damage in Crystals, Methuen, London, 1965.
[30] G. Szenes, Information provided by a thermal spike analysis on the microscopic processes of track formation. NIM-B 2002, in press.
[31] L.T. Chadderton, D. Fink, Fullerene genesis by ion beams III. On the absence of latent tracks in GeV ion irradiated graphite, Radiat. Eff. Defects 152 (2000) 87–107.
[32] L.T. Chadderton, paper read at the conference Radiation Effects in Insulators - 11, Lisbon, September, 2001, On selection rules of crystals for latent particle track registration, to be published, NIM-B.
[33] T.A. Paul, P.G. Fitzgerald, Transmission electron microscopic investigations of fission tracks in fluorapatite, Am. Mineral. 77 (1992) 336–344.
[34] A.V. Nazorov, M.G. Ganchenkova, A.A. Mikheev, Theory of diffusion under pressure, Defect Diffus. Forum 194-1 (2001) 49–54.
[35] L.T. Chadderton, Nucleation of damage centers during ion implantation of silicon, Radiat. Eff. 8 (1971) 77–85.
[36] R.A. Wolf, K.A. Farley, L.T. Silver, Helium diffusion and low-temperature thermochronometry of apatite, Geochim. Cosmochim. Acta 60 (1996) 4231–4240.